The Transverse Tensile Properties of Boron Fiber Reinforced Aluminum Matrix Composites

K. M. PREWO AND K G. KREIDER

The transverse tensile properties of boron fiber reinforced aluminum have been determined as a function of fabrication parameters, matrix alloy and fiber types, fiber content, specimen geometry, and thermal environment. Matrix alloys investigated include 2024, 6061, 5052, 5056, 2219, 1100, and Al-7 pct Si. The fibers investigated include 4.0 mil boron, 4.2 mil BORSIC , R.F. boron, 5.6 mil boron, 5.7 mil BORSIC, and 4.0 mil silicon carbide. It was shown that the composite transverse tensile performance is a function of all of these variables and that transverse strengths of up to 45,000 psi can be achieved by the choice of the proper combination of matrix, fiber type and fabrication procedures.

THE boron-aluminum composite system is very attractive as a structural engineering material because of its outstanding modulus and strength ratios.[1] For this reason engineering applications such as turbine engine fan blades,[2-4] reinforced stiffened panels and airframe structural beams,[5] have been developed. Boron-aluminum composites have also been chosen because of the excellent high temperature (600°F) properties[6] and joinability.[7]

These excellent properties are basically related to the reinforcing fiber properties while the strength in unreinforced directions is more closely related to the matrix properties. Although a unidirectional 50 pct by volume boron-aluminum composite can exhibit a longitudinal ultimate tensile strength of 200,000 psi, the transverse strength is generally less than one-tenth of this value.[1,5,8-11] This is in contrast to the ratio of axial to transverse elastic moduli of less than two to one. A method for circumventing this strength problem has been to cross ply layers of composite to provide the axial strength of fibers in more than one direction. This, however, is not always a satisfactory solution because of the resultant compromise in properties. It has been the goal of this investigation to determine the transverse tensile properties of boron-aluminum composites and to elucidate composite failure mechanisms to permit the development of a method for increasing transverse strength. Silicon carbide coated boron fiber has been used in this investigation primarily because of its greater chemical stability than uncoated boron in aluminum matrices.[12]

EXPERIMENTAL METHOD

1) Materials

The major portion of composite material fabricated for this research program contained 4.2 mil diam BORSIC fiber. Additional tests were also performed using 4.0 mil boron, 5.6 mil boron, 8.0 mil boron, 5.7 mil BORSIC, and 4.0 mil silicon carbide fibers. Boron fiber is produced by the vapor deposition of boron onto a heated tungsten substrate. Fibers produced using dc and rf heating techniques were both evaluated. The BORSIC fiber is fabricated by depositing a 0.1 to 0.15 mil coating of silicon carbide onto the boron. The silicon carbide fiber is also produced by deposition onto a tungsten substrate.

The matrix materials used were all aluminum base alloys. Three heat treatable alloys, 2024, 2219, and 6061 were used as well as three nonheat treatable alloys, 1145/1100, 713/528, and 5052/5056. The matrix consisted of 1 mil thick foils and plasma sprayed material. A single exception to this is the 2219 matrix which consisted solely of plasma sprayed material. The 5052/5056, 713/528, and 1145/1100 designations refer to foil/plasma spray combinations of two different alloys to make up the composite matrix. Nominal alloy compositions are presented in Table I.

2) Matrix Material Fabrication

Specimens fabricated solely of aluminum matrix alloys, without fiber reinforcement, were prepared by first plasma spraying alloy powder onto 0.001 in. thick foil to produce metal tapes. Layers of these tapes were then hot press diffusion bonded under conditions of temperature and pressure equal to those used to produce fiber reinforced composites having the same matrices. Resultant specimens were approximately 65 to 75 pct plasma sprayed material. This percentage of plasma sprayed material agrees with a similar fraction of the matrices (not fraction of total composite) of the fiber reinforced composites. The 2219 material was made

Table I. Matrix Alloy Compositions

Designation	Wt Pct of Element				
	Cu	Mg	Mn	Si	Al
1100	–	–	–	–	99.0
1145	–	–	–	–	99.45
2024	4.5	1.5	0.6	–	Bal
2219	6.3	–	0.3	–	Bal
6061	0.25	1.0	–	0.6	Bal
5052	–	2.5	–	–	Bal
5056	–	5.2	0.1	–	Bal
713	0.25	0.10	–	7.5	Bal
528	–	–	–	7.7	Bal

K. M. PREWO and K. G. KREIDER are Research Scientist and Program Manager, respectively, Composite Materials, United Aircraft Research Laboratories, East Hartford, Conn.

Manuscript submitted November 18, 1971.

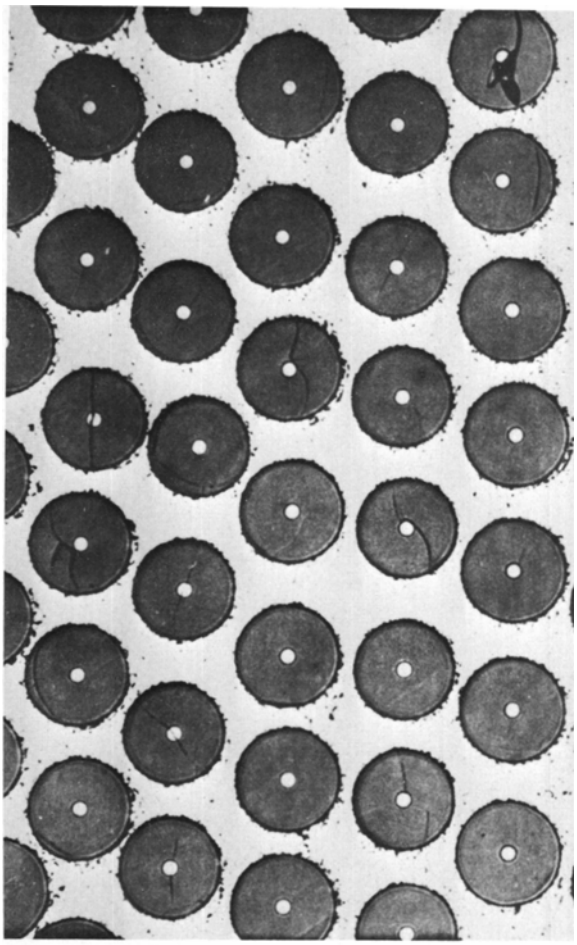

Fig. 1—4.2 Mil BORSIC-6061 aluminum composite microstructure.

solely of plasma sprayed alloy. Tensile specimens were machined to have 1.25 in. long gage lengths and were tested at a crosshead velocity of 0.01 ipm using a Tinius-Olsen tensile tester.

3) Composite Fabrication

The composites were fabricated by hot press diffusion bonding of plasma-sprayed monolayer tapes. The filament winding operation is performed on a modified lathe, using a screw-thread auger to control the fiber spacing. The aluminum foil wrapped mandrel which receives the winding is spring loaded to allow for thermal expansion mismatch between the aluminum foil substrate and the fiber. Plasma-spray fabrication was done in argon. The cylindrical mandrel, covered with a layer of aligned filament, is rotated and traversed before a plasma arc to deposit an even layer of matrix alloy. Aluminum alloy powder is then injected into the hot gas of the plasma arc and melted in the exothermic or recombination zone. The molten aluminum droplets are impacted on the foil and fiber and quickly solidified, bonding the monolayer tape together.

The hot press diffusion bonding of layers of plasma sprayed tape to form 1 by 5 in. plates was performed primarily at temperatures within 100°F of the matrix alloy solidus temperature at pressures of greater than 5000 psi in an argon atmosphere. Lower temperatures of bonding, however, were found to be necessary when composite specimens were fabricated containing boron fiber. These lower temperatures prevented degradation of boron filament strength by reaction with the aluminum matrix. Neither the BORSIC nor silicon carbide fibers were susceptible to degradation at temperatures used for fabrication.[12] Selected composite specimens were heat treated to the T-6 condition subsequent to fabrication.

A microstructure typical of composites fabricated by the above procedure is presented in Fig. 1. The specimen shown contains approximately 50 pct BORSIC fiber by volume. Specimens were also fabricated containing other percentages of fiber. These specimens were produced by the same procedures as given above and filament distribution was controlled to maintain a nearly hexagonal fiber array.

4) Composite Specimen Preparation and Testing

The diffusion bonded composite plates were cut into 0.25 in. wide, 5 in. long parallel sided tensile specimens. Cutting from the plates was performed primarily by use of a diamond abrasive wheel; however, some specimens were also prepared using electrodischarge machining techniques to compare the effects of cutting techniques. Strain gages were mounted on both sides of each specimen to determine modulus and strain to failure. The specimens were aligned in grips by use of a X12.5 microscope and a specially designed alignment jig. This was done in such a way as to leave a 1 in. long gage length between grips. The gripped specimens were then aligned in a Tinius-Olsen tensile tester and strained at a strain rate of 0.01 ipm.

Measurements of the transverse elastic modulus at elevated temperature were performed using two different techniques of measurement. The first method was to use elevated temperature strain gages and to tensile test the gaged specimens at temperature. The second method was a dynamic determination of the modulus that is frequently referred to as the "free-free beam" technique and relies on the measurement of the resonant vibrational frequencies of composite specimens excited at temperature.[13-17]

Several BORSIC-6061 composite specimens were tested in transverse compression. These specimens were 0.5 in. in height, 0.18 by 0.12 in. in cross section and were strain gaged to determine modulus and stress-strain behavior.

The effects of edge condition on composite transverse tensile performance have been demonstrated by the use of transverse tensile specimens having the BORSIC fiber ends free of matrix. This was accomplished by etching away at least 0.25 in. of aluminum from both edges of 1 by 5 in. composite plates. The resultant specimens had 0.25 in. long matrix free fiber ends protruding from each side. A typical specimen is shown in Fig. 2.

RESULTS AND DISCUSSION

1) Matrix Material

The results of tensile tests performed on the plasma sprayed plus foil matrix alloys are given in Table II. In all cases the final processing step for these materials was a slow cool in the hot press dies from the

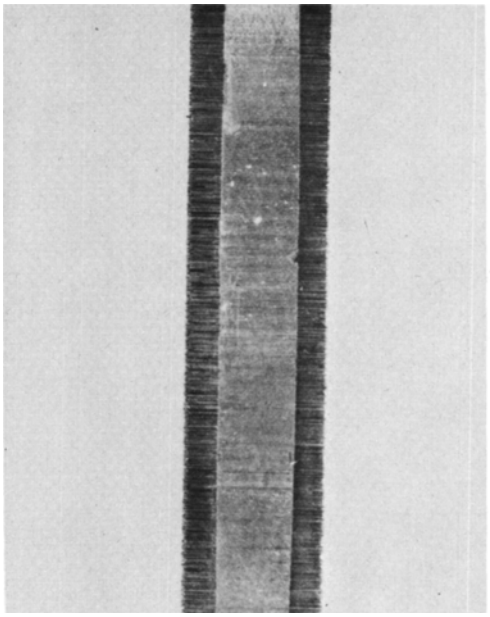

Fig. 2—Free fiber end tensile specimen.

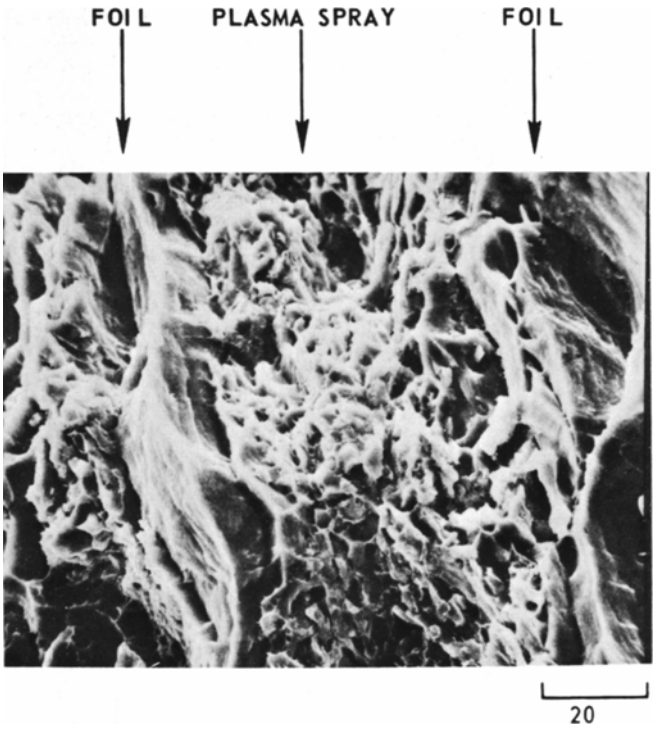

Fig. 3—Matrix material fracture surface.

Table II. Experimentally Determined Properties of Plasma Sprayed Material with Foil in the As-Fabricated (F) Condition

Alloy	Elastic Modulus 10^6 psi	Yield Stress at 0.2 Pct Offset 10^3 psi	Ultimate Tensile Strength, 10^3 psi	Strain to Fracture, 1.25 In. Gage Length
6061	10.2	11.2	19.6	16 pct
2024	10.4	18.6	35.0	13 pct
1100-1145	9.1	6.2	12.5	20 pct
Al-7 pct Si	10.5	9.4	17.5	23 pct
2219 (no foil)	9.6	14.4	27.6	12 pct
5052/56	9.8	19.5	38.6	13 pct

Typical Properties of Wrought Material in the Annealed Condtion*

Alloy	Yield Stress 10^3 psi	Ultimate Tensile Strength, 10^3 psi	Strain to Fracture, 2 In. Gage Length
6061	8.0	18.0	25 pct
2024	11.0	27.0	20 pct
1100	5.0	13.0	35 pct
2219	10.0	25.0	20 pct
5052	13.0	28.0	25 pct
5056	22.0	42.0	35 pct

*Properties, Physical Metallurgy and Phase Diagrams, Aluminum, Vol. 1, Kent R. Van Horn, ed., 1967.

pressing temperature. Resultant specimens are in a fully annealed as-fabricated condition designated as the F condition. For this reason the data reported can be compared best with the properties of wrought materials of similar composition in the fully annealed condition. Such a comparison reveals that the elastic moduli of the composite matrix materials are approximately equal to those of wrought material. This equality is evidence that the specimens tested were fully consolidated by the diffusion bonding procedures used. As has been shown in the past for monolithic materials,[18,19] the elastic modulus is a sensitive function of void content of materials and even small percentages of voids present would have caused the measured moduli to be considerably less than those measured. The comparison of strengths reveals that the yield and ultimate tensile strengths of the composite matrices are greater than those of the wrought material. The strains to fracture are 30 to 40 pct less than those of wrought material.

This higher strength and lower ductility can be related to the very fine dispersions of precipitate produced by the plasma sprayed structure. Oxides present on the powder used in the plasma spray process also will contribute to this increase in strength. Polished sections of these alloys display the precipitate and oxide dispersions. The microstructural features of the plasma sprayed material are considerably finer than those of the adjacent foils. This is reflected in the morphology of the fracture of the plasma sprayed material as compared to the foil, Fig. 3. The plasma sprayed material has undergone large amounts of local plasticity and dimpling associated with the fine dispersions. Another reason for the lower ductility herein reported may be due to the fact that the specimens tested during this investigation were all less than 0.1 in. in thickness. Kaufman and Davies[20] have shown that the fracture strain of sheet aluminum specimens is extremely sensitive to specimen thicknesses below 0.1 in. A 6061 alloy was shown by the authors to exhibit a failure strain of less than 12 pct when tested at below 0.1 in. in thickness while a 0.4 in. thick specimen failed after 18 pct elongation.

Tensile tests at 400° and 600°F also have been performed on these matrix materials. The data obtained for the 2024 and 6061 aluminum alloys are presented in Fig. 4. In all cases the specimens were held at the test temperature for 30 min prior to testing. The effect of heat treatment on matrix strength is also shown in the figure. For both the 6061 and 2024 alloys, a standard T-6 heat treatment increased the room temperature tensile strength substantially above the levels of the as-fabricated material. This difference became

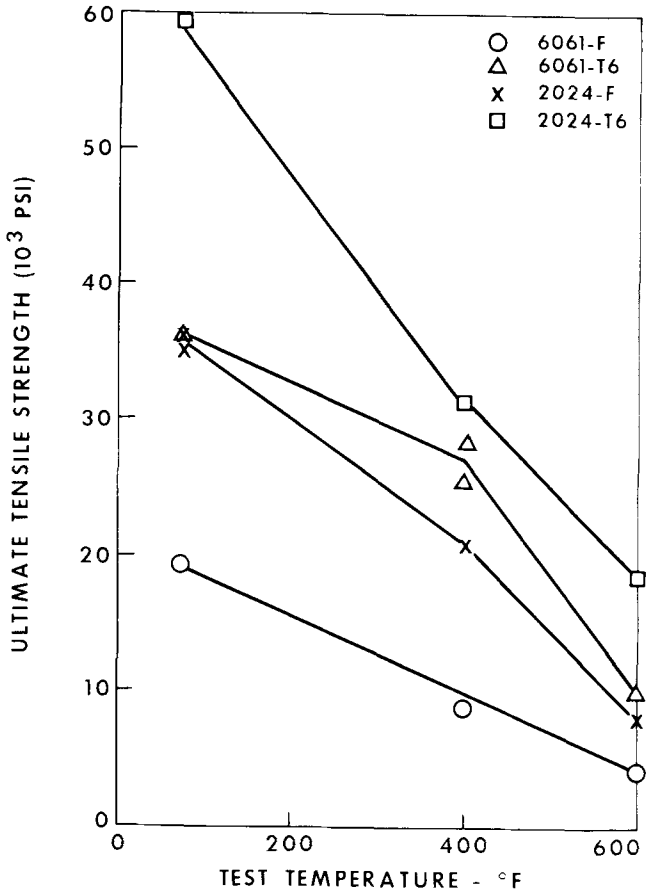

Fig. 4—Ultimate tensile strength of plasma sprayed plus foil matrix material as a function of temperature.

smaller at the elevated temperatures due to rapid overaging of the alloys. Comparison of the data in the two figures indicates that the 2024 matrix material is capable of higher strengths than the 6061 material over the entire temperature range of testing.

2) Composite Transverse Elastic Modulus

The variation of composite transverse elastic modulus with BORSIC fiber content is presented in Fig. 5. The modulus increases with increasing volume fraction fiber. However, as pointed out by others[9,21-24] a simple "rule of mixtures" approach that disregards filament packing array is not applicable to an analysis of transverse properties. Microstructural examination of the specimens tested in this investigation indicate that filament packing is best described in terms of a nearly hexagonal array and the data obtained agree best with theoretical analysis based on this type of fiber distribution.

The results of transverse elastic modulus determinations at elevated temperature indicate that the modulus decreases with increasing test temperature and at 600°F the modulus is 10 to 20 pct less than the room temperature value. Fig. 6 presents the data for both methods of modulus determination used. This decrease in modulus is due, in a large measure, to the decrease in modulus experienced by the matrix material over this same temperature interval. This can be seen from the data shown in Fig. 6 for the elastic modulus of a typical plasma sprayed plus foil matrix material pre-

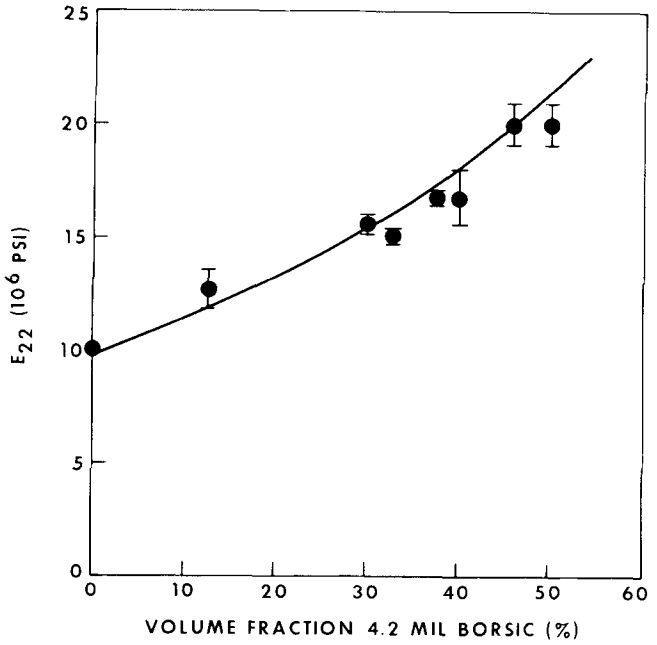

Fig. 5—Composite transverse elastic modulus as a function of fiber content.

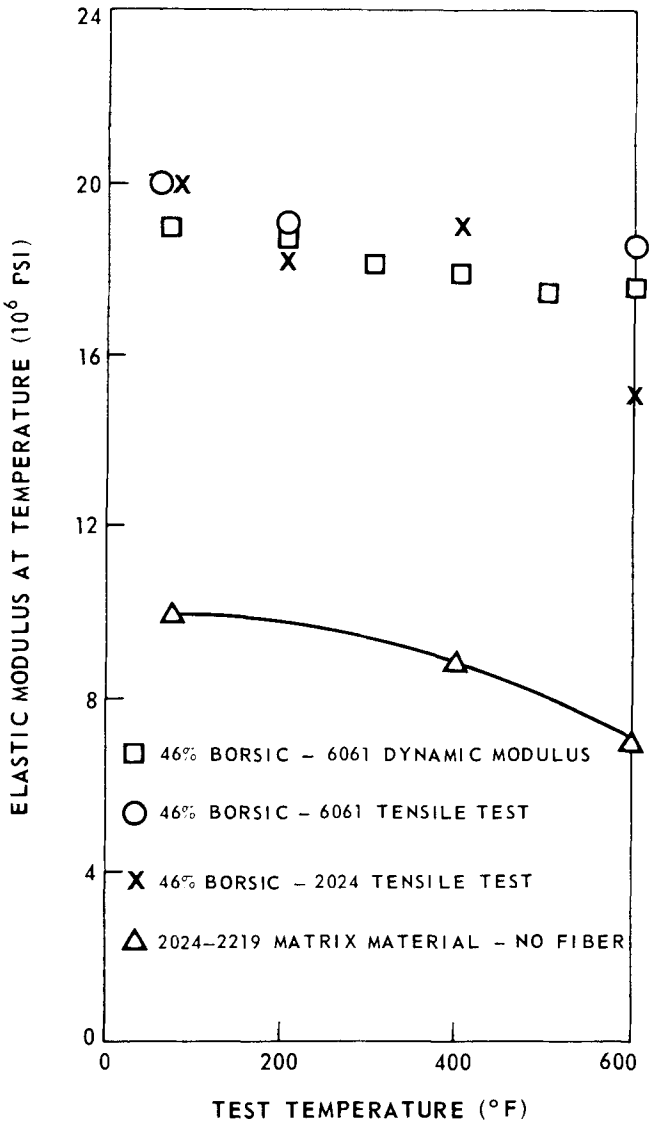

Fig. 6—Transverse elastic modulus as function of temperature.

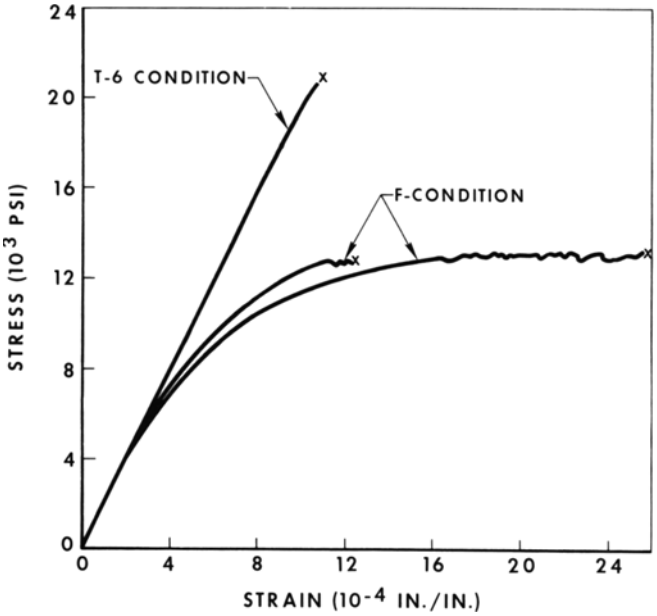

Fig. 7—46 pct 4.2 mil BORSIC-6061 aluminum 90 deg tensile stress strain curves. F indicates as fabricated, and T-6 indicates heat treated conditions.

pared by hot pressing and tested in tension at elevated temperature. At 600°F the modulus has reached the value of 7×10^6 psi in agreement with the value expected for a wrought material of the same composition.[25] This decrease in matrix modulus of 30 pct can cause a major portion of the decrease in composite modulus observed. The elastic modulus of the BORSIC fiber is also decreasing with increasing temperature;[26,27] however, little data is available in the temperature region of 600°F to obtain a reliable value. The data of Metcalfe and Schmitz[26] indicate an elastic modulus of 50×10^6 psi for boron at approximately 600°F. Using this modulus for the BORSIC fiber and a modulus of 7×10^6 psi for the matrix, the work of Adams and Doner[21] would indicate that a modulus of approximately 18×10^6 psi would be expected. This is in fairly good agreement with the values obtained as shown in the figure.

The transverse elastic modulus measured during compression testing at room temperature was found to be 18×10^6 psi. The specimen tested contained 46 pct vol fraction 4.2 mil BORSIC fiber. The elastic modulus as measured in compression is in substantial agreement with that measured in tension.

3) Transverse Tensile Strength and Failure Strain

Transverse tensile stress-strain curves for 4.2 mil BORSIC-6061 matrix composites are shown in Fig. 7. Both as-fabricated (F) and heat treated (T-6) composite behavior are illustrated. Composite yielding occurs at a level of approximately 4000 psi in the F condition while in the T-6 condition the curve is linear nearly to the point of failure. The tensile strengths in both conditions are considerably lower than those of the unreinforced matrix, however, a major strength increase has been realized by the use of the heat treatment procedure. Although the form of the stress-strain curve was considerably altered by heat treatment, the composite failure strain and transverse elastic modulus were not.

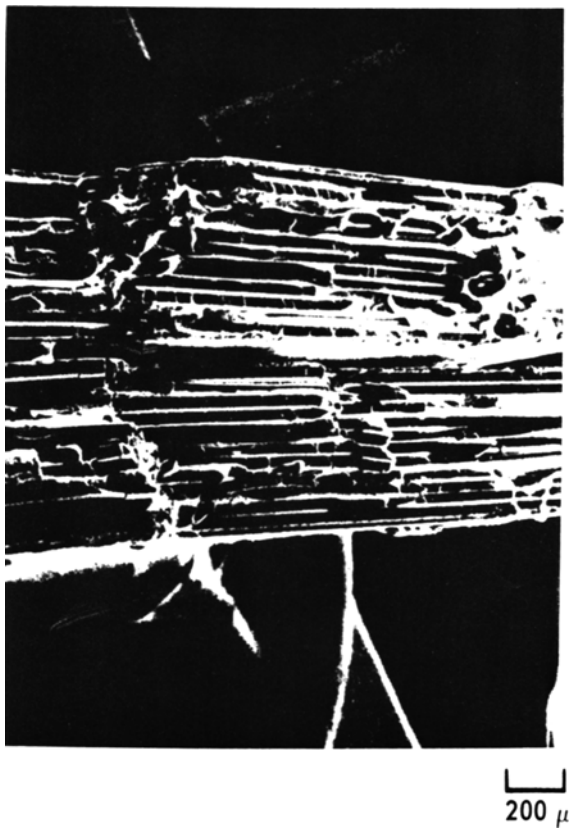

Fig. 8—Fracture surface of 50 pct by volume 4.2 mil BORSIC-6061 transverse tensile specimen.

Two different types of stress-strain curves were generated by the F condition composites that were manufactured and processed under identical conditions. The initial portions of the curves were similar; however, for some specimens tested, fracture occurred at a strain of approximately 0.0012 in. per in. while for others the strain to fracture was twice this amount. The specimens which fail at the larger strain exhibit a region of increasing strain under nearly constant stress and frequently fracture in a region directly under the strain gages on the specimen surface. Thus, this phenomenon may be associated with the location and propagation of failure through the specimen. Curves similar to this second type (larger strain to failure) have been observed by others as reported by Adams.[28]

The fracture process in transverse tension of BORSIC-6061 specimens was examined more closely to determine the failure mechanism. In general, composite failure initiated at the specimen edges and propagated by a combined mode of matrix failure and fiber splitting. A typical composite fracture surface is shown in Fig. 8. In the figure, taken by scanning electron microscopy, the fiber cores appear as white lines and every fiber in the cross section has failed on a diametral plane. A higher magnification examination of split fibers, Fig. 9, reveals that the fiber fracture surfaces consist of two different fracture modes. One-half of each fiber diametral plane is smooth while the other half is rough. This is due to initial fracture of the fiber at a preexistent flaw in the smooth region,[29] followed by crack propagation across the boride core and reinitiation of fracture in the boron of the rest of the fiber causing the jogged fracture surface.

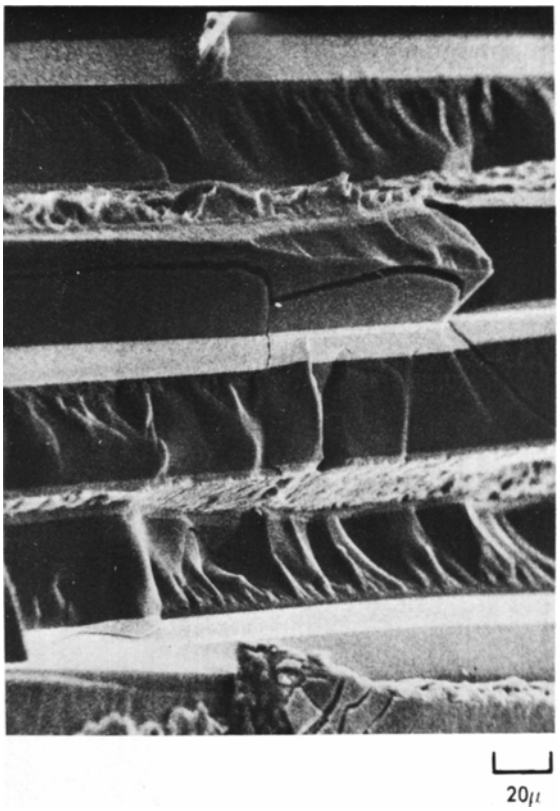

Fig. 9—Fracture surfaces of longitudinally split 4.2 mil BORSIC fibers.

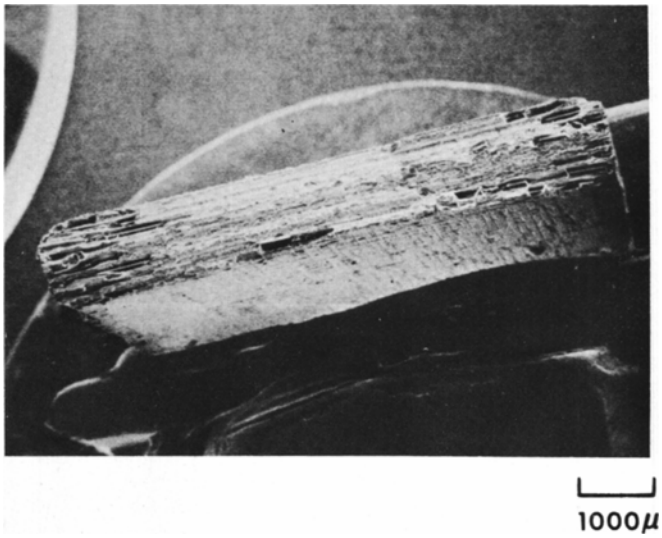

Fig. 10—Fracture surface of a 48 pct vol fraction 4.2 mil BORSIC-1145/1100 transverse tensile specimen.

The behavior of 48 pct-4.2 mil BORSIC-1145/1100 composites differed considerably from the above described 6061 matrix composites. Composite strength is 11,500 psi, which is less than that of the 6061 matrix composites; however, the composite failure strain is 0.4 pct for composite failure away from the strain gages. This value is considerably higher than the highest values obtained for the 50 pct-4.2 mil BORSIC-6061 composites tested. The transverse elastic modulus is 22×10^6 psi, which approximately equals that of the 6061 matrix composites. Examination of the fracture surfaces of the 1145/1100 matrix specimens tested revealed that very little fiber splitting accompanied composite failure, Fig. 10. Only the regions near the edges of the transverse fibers are split. This splitting corresponds to damage introduced to the fibers during specimen preparation. The specimens were cut from larger plates of material by the use of a diamond abrasive wheel. As will be discussed in a later section of this paper, the action of the abrasive wheel is sufficient to damage the BORSIC filaments. The primary fracture mode observed is one of matrix rupture. Micropore opening and coalescence similar to that found in monolithic aluminum is present and very little evidence of aluminum matrix-fiber debonding was observed.

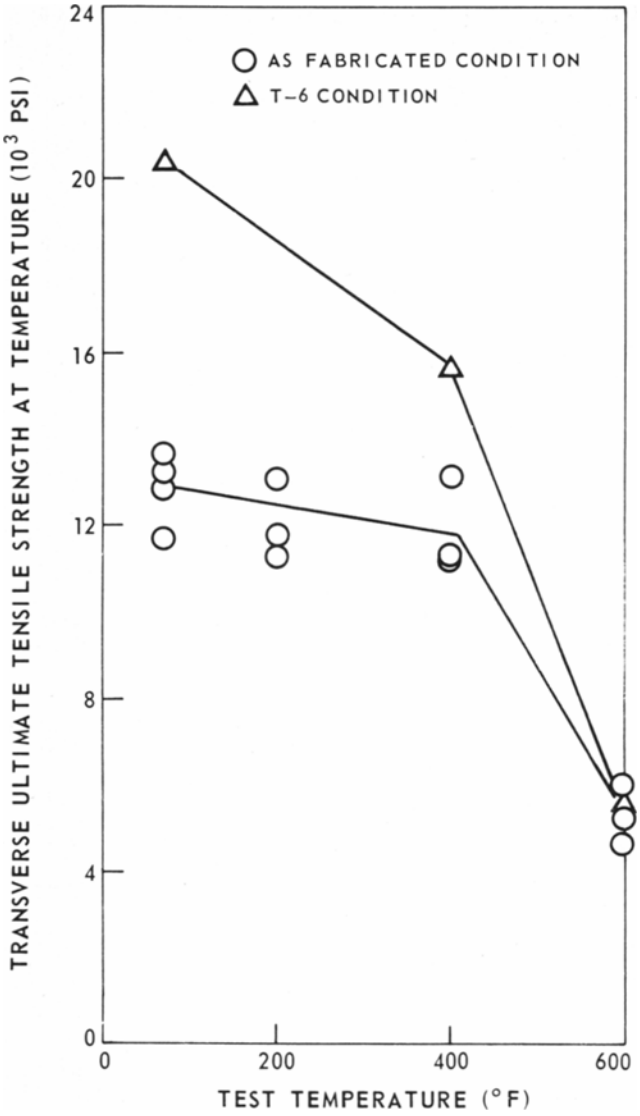

Fig. 11—Transverse tensile strength of 4.2 mil BORSIC-6061 aluminum as a function of test temperature.

The results of the transverse tensile testing of 4.2 mil BORSIC-6061 and 2024 matrix composites at temperatures between 70° and 600°F are presented in Figs. 11 and 12. As discussed previously, the T-6 heat treatment increases the transverse strength above that of the as-fabricated composite. This difference becomes smaller with increasing test temperature as the overaging of the heat treated material takes place. At room

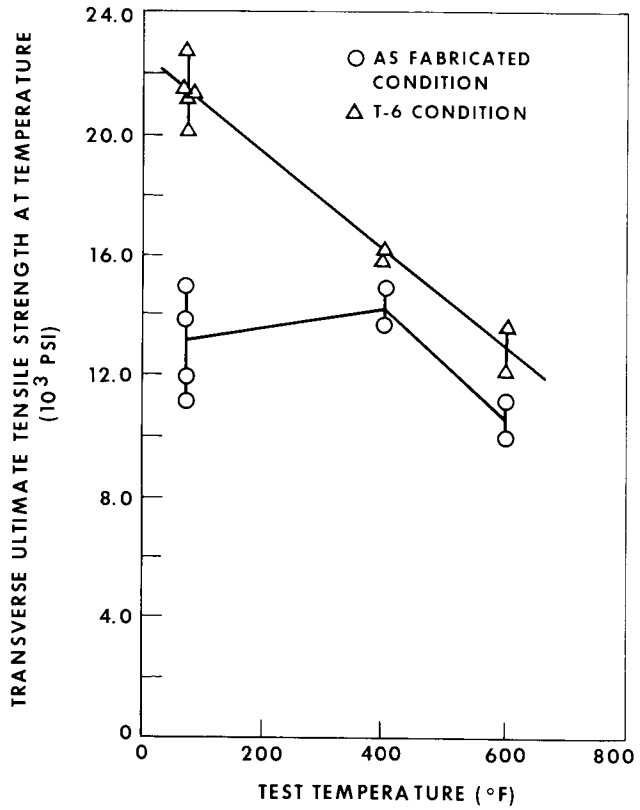

Fig. 12—Transverse tensile strength of 4.2 mil BORSIC-2024 aluminum as a function of test temperature.

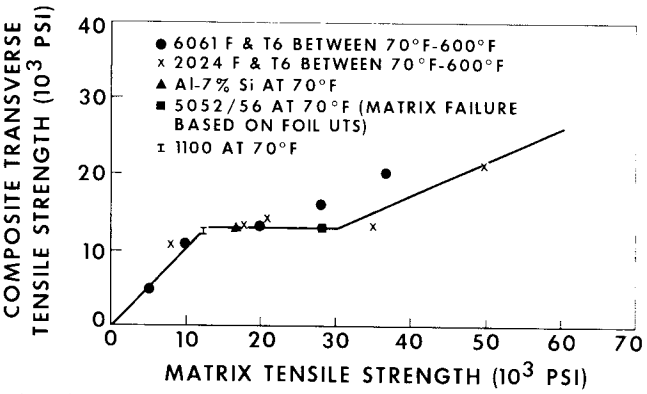

Fig. 13—Transverse tensile strength of 50 pct by volume 4.2 mil BORSIC-aluminum as a function of unreinforced matrix strength.

temperature the strengths of the 2024 and 6061 matrix composites are approximately equal. As the test temperature is increased the 2024 composite retains a higher strength level than the 6061. This is in agreement with the unreinforced matrix properties presented in Fig. 4 where the 2024 alloy exhibited higher elevated temperature strength than the 6061 material. A comparison of the data obtained for composite transverse strength with the unreinforced matrix strength reveals that for both 6061 and 2024 matrix materials, the difference between matrix strength and composite strength decreases with increasing temperature.

The fracture surfaces of the composites tested were examined to determine the mode of fracture. As discussed earlier, at room temperature all of the fibers in the composite fracture surface were split longitudinally. This changed, however, as the test temperature increased. With increasing temperature of test, the fraction of fracture surface occupied by split fibers decreased. In the case of the 6061 matrix composites, at 600°F no fiber splitting was found to occur and instead the mode of fracture corresponded to that of matrix failure. None of the fracture surfaces studied exhibited evidence of fiber-matrix debonding as a primary mode of fracture.

A summary of the transverse tensile strength of 50 pct-4.2 mil BORSIC fiber reinforced composites as a function of matrix strength is presented in Fig. 13. The data include five different matrices, two of which are in both as-received and heat treated conditions, as well as data obtained over the test temperature range of 70° to 600°F. Three distinct regions of behavior are seen to occur and are depicted in the figure.

REGION I

The fracture surfaces of the failed composites exhibited only small amounts of split fibers. In this region the composite strength is approximately equal to the matrix strength. Thus, in this region the matrix fails at an applied composite stress below that necessary for fiber failure. The behavior of the 1100 matrix composites at room temperature and the 6061 matrix composites at elevated temperature are characteristic of this region. The fracture surface presented in Fig. 10 is typical of these composites. The observed equality of composite and matrix strength in this region is in agreement with the predictions of Lin *et al.*[9,10] based on the von Mises-Hencky distortional energy criterion for yielding.

REGION II

In this region of matrix strength the composite transverse tensile strength is substantially independent of matrix strength. Fracture surfaces are characterized by the presence of large amounts of fiber splitting, Fig. 8. In this region the matrix strength is sufficient to cause loading of the fibers to their ultimate transverse strength prior to composite failure. Adams[28] has analyzed in detail the stress distribution of boron aluminum during transverse tension and pointed out the existence of significant stress concentrations in the fiber which may contribute to fiber failure in this regime. Upon fiber failure, however, the remaining composite matrix material also fails immediately due to overload. The remaining matrix does not have the load carrying capability to prevent total composite failure subsequent to fiber failure. Thus, the constancy and level of composite strength in Region II and the points of transition between Regions I and II, and II and III are controlled by the fiber transverse tensile strength. A higher transverse tensile strength fiber would raise the composite strength level of the Region II plateau and also raise the matrix strength levels of the transition points between regions. Examples of this will be presented in later sections of this report.

REGION III

In Region III, as in Region II, matrix strength is sufficient to cause transverse fiber failure prior to composite failure; however, matrix strength is also high

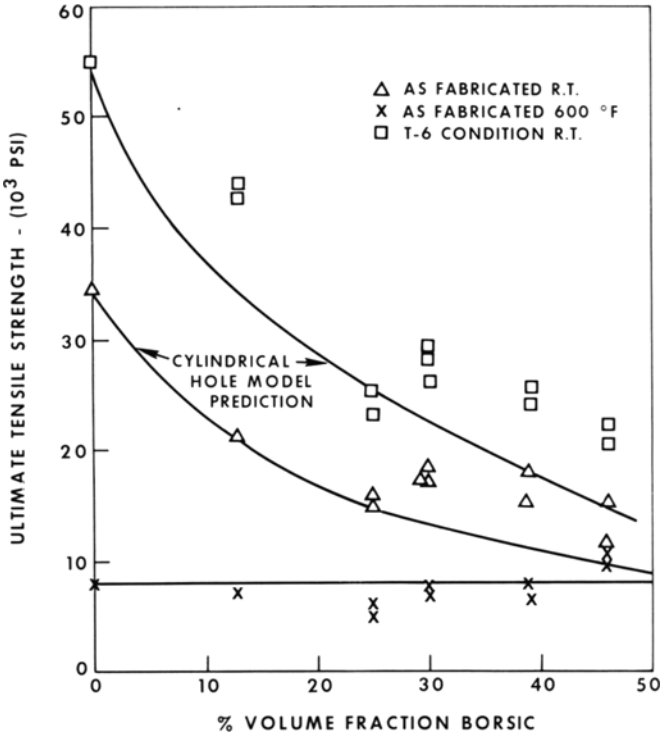

Fig. 14—Transverse tensile strength as a function of volume fraction 4.2 mil BORSIC fiber in 2024 aluminum.

enough to prevent immediate overload failure. Thus, the composite strength is determined by the net section of load bearing matrix left, subsequent to fiber splitting, and the strength of this matrix. In the case of the heat treated composites, the presence and magnitude of residual stresses, no doubt, is also of importance. Fracture surfaces are typically similar to that shown in Fig. 8.

It should be noted that the data for the 5052/56 matrix composite was presented in Region II rather than in Region III. This matrix material contains both a foil of 5052 aluminum with a tensile strength of 28,000 psi and the plasma sprayed material of 5056 with a tensile strength of 42,000 psi. After fiber splitting occurs the major portion of the load carrying matrix consists of the weaker 5052 foil due to the fact that the foil (or tape) plies are aligned parallel to the transverse tensile axis. Thus, the residual effective matrix strength for this composite is actually 28,000 psi which puts it in Region II.

The results of tests performed on 0 to 46 pct BORSIC-2024 composites are presented in Fig. 14. For both the as-fabricated condition and T-6 condition, when tested at room temperature, the tensile strength decreases with increasing volume fraction fiber. At 600°F, however, the transverse strength is substantially independent of fiber volume fraction. The values of ultimate tensile strength used for the unreinforced matrix were obtained by testing plasma sprayed plus foil material as described in the section on matrix properties. The lines drawn in Fig. 14 from the two 70°F unreinforced matrix strength data points do not represent a fit to the composite data but instead are a result of calculations performed using a simple model. In this model, it was assumed that the fibers had been removed from the composite leaving a network of cylindrical holes. The composite strength was then

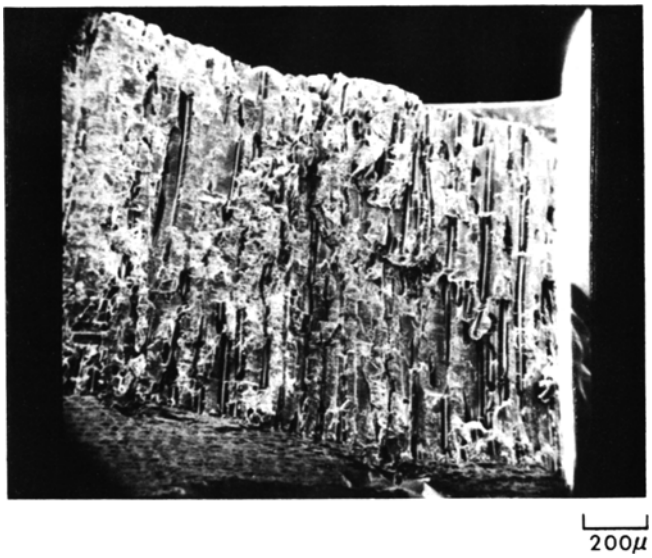

Fig. 15—Fracture surface of 4.2 mil BORSIC-6061 transverse compression specimen.

calculated on the basis of the net minimum cross-sectional area remaining. Little difference in strength was found between the square or hexagonal hole arrays and composite strength is expected to be only 20 pct of that of the unreinforced matrix for 50 pct fiber content specimens. In both the as-fabricated and T-6 conditions, the composite strengths measured were found to be in excess of those calculated.

The difference in Fig. 14 between composite behavior at room temperature and at 600°F can be related to differences in fracture mode. At room temperature the fracture surfaces are characterized by longitudinal splitting of all the fibers in the fracture surface. Composite behavior at room temperature is similar to that described in Fig. 13 for Region II and III. At the high volume fractions of fiber, in the F condition, the matrix is overloaded by local fiber failure as was described for Region II. Matrix load carrying capability is increased by decreasing fiber content and composite heat treatment so that increasing composite strength can be achieved, typical of Region III. At 600°F, however, the amount of fiber splitting is far less and in some cases no fiber splitting at all is found. The failure occurs completely through the matrix. For this latter case of matrix failure the observation that composite strength is independent of volume fraction fiber is again consistent with the prediction of Chen and Lin[9] and corresponds to Region I in the previous analysis. It is also clear, however, that this prediction does not hold for the tests performed at room temperature. This is due to the fiber mode of failure being operative at room temperature.

4) Compression Testing

The transverse compression tests were performed on 6061 matrix composite specimens containing 46 pct BORSIC fiber. The room temperature transverse compression stress-strain curve exhibited an elastic modulus approximately equal to that measured in transverse tension, however, the maximum load carrying capability is considerably greater than that in tension. After approximately 6 pct strain and at a

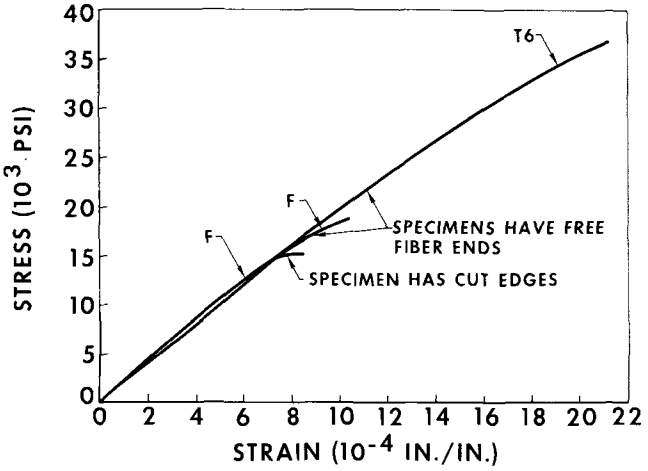

Fig. 16—46 pct 4.2 mil BORSIC-2024 aluminum 90 deg tensile stress strain curves. F indicates as-fabricated and T-6 indicates heat treated conditions.

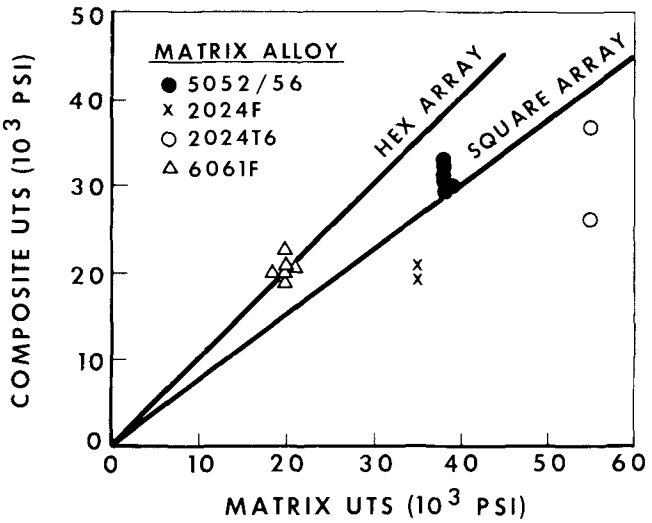

Fig. 17—Transverse tensile strength of free fiber end specimens containing 46 pct by volume 4.2 mil BORSIC fiber.

stress of 37,900 psi the load began to decrease with increasing strain. The cause of this decrease was the shear failure of the specimen. At 600°F the specimens failed by the same mechanism, however, the maximum stress was 9500 psi. The fracture surface of a room temperature specimen is shown in Fig. 15. As can be seen in the figure, fiber splitting is once again characteristic of the fracture surface. Also visible is evidence of large amounts of shear deformation of the aluminum between the split fibers.

5) The Effects of Transverse Tensile Specimen Configuration on Composite Performance

Transverse tensile failure commonly initiates at the edges of the composite specimens, this behavior is associated with the damage introduced to the specimens during specimen cutting and preparation. Specimens tested during this study were cut from larger composite plates using diamond abrasive wheel, electrodischarge machining (EDM), and diamond abrasive wheel cutting followed by mechanical polishing. All exhibited similar stress strain behavior. These three techniques resulted in fiber damage sufficient to initiate composite failure and no significant variation in transverse strength was realized.

Significant changes in composite stress strain behavior could be obtained, however, by testing free fiber end specimens of the type depicted in Fig. 2. The stress-strain curves obtained by tensile testing BORSIC-2024 composite specimens of this configuration are shown in Fig. 16. A stress-strain curve characteristic of the more conventional type of transverse tensile specimens having cut edges is also included in the figure for comparison. It is seen that the specimens with the free and cut configurations exhibit the same elastic modulus; however, the tensile strength and strains to fracture of these composites differ substantially. For the as-fabricated (F) condition, the "cut-edges" composite exhibits a transverse tensile strength of 15,000 psi while the "free-end" composite is capable of 19,000 psi. In the T-6 condition, the "free-end" composite fails at 36,000 psi, while the tensile strengths of "cut-edge" composites having the same matrix and undergoing the same heat treatment have been shown in this paper to be only 22,000 to 24,000 psi. Thus, when the fiber edges of these composites are unstressed, the transverse tensile strength increases substantially.

Fig. 17 illustrates the tensile strengths obtained by testing "free-fiber-end" 90 deg specimens. In the figure, the composite tensile strength is plotted as a function of the ultimate tensile strength of the unreinforced matrix. The lines drawn indicate the tensile strengths to be obtained if composite behavior agreed with the analysis of Chen and Lin[9]. Strengths expected for both square and hexagonal fiber arrays are represented. This figure is in marked contrast to one having similar axes reported earlier in Fig. 13 for cut-edge composites. In that figure it was shown that composites having 2024, 6061, and 5052/56 matrices all exhibited the same transverse strength when tested in the as-fabricated condition at room temperature. For the data reported in Fig. 17 this is no longer the case. The transverse strength of the composites tested is not constant and is dependent on matrix strength. The composites having the 5052/56 matrix material exhibited tensile strengths of approximately 30,000 psi while those having a 6061 matrix failed at only 20,000 psi. For all of these composites, the fracture surfaces of the tested specimens exhibited some fiber splitting, however, the fiber splitting observed was substantially less than that reported above when the specimen edges were in the cut condition. The specimens tested in the free end condition with a 2024 aluminum matrix were found to exhibit larger amounts of fiber splitting. This is probably why the composite tensile strengths reported in Fig. 17 for these specimens were not equal to the full matrix strength.

Several transverse tensile specimens were tested with fiber ends protruding less than 0.25 in. beyond the matrix edge. No change in fracture mode or tensile strength was noted from that of cut edge specimens. This was found to be due to the fact that fiber edge damage extended up to 0.25 in. from the fiber ends. In a similar manner, some specimens were found to exhibit fiber damage to greater than 0.25 in. so that matrix removal would have to extend much further into the specimens to provide increased performance.

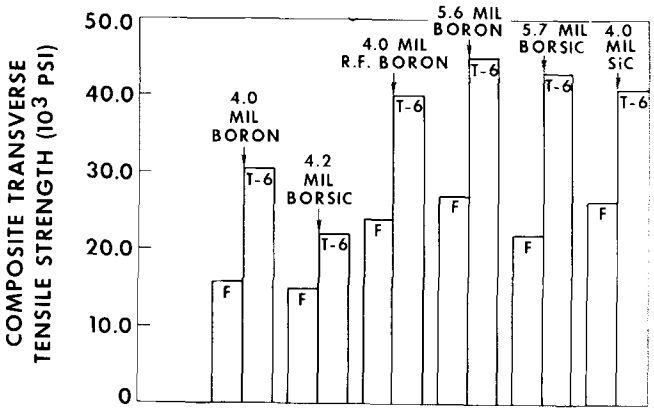

Fig. 18—Transverse tensile strength of 2024 aluminum matrix composites as a function of fiber type (40 to 50 pct fiber content).

6) Dependence of Composite Transverse Tensile Strength on Fiber Type

It has been shown, in the foregoing sections, that the transverse tensile strength of BORSIC-aluminum composites is dependent upon the splitting tendency of the reinforcing fibers. To further illustrate this point the transverse tensile strength of 2024 matrix composites was examined as a function of fiber type. The data are presented in Fig. 18 for both as-fabricated and heat-treated specimens. The comparison of composite strengths reveals that several different fibers are capable of providing composite strengths in excess of 40,000 psi. In every case these composites did not exhibit significant amounts of fiber splitting on their fracture surfaces. These superior fibers include R. F. boron, 5.6 mil boron, 5.7 mil BORSIC and silicon carbide. Fibers that exhibited major amounts of fiber splitting, 4.0 mil boron and 4.2 mil BORSIC, provided considerably weaker composites.

The reasons for the superior performance and lower splitting tendency of some of the fibers tested relate to their fabrication and resultant residual stress state. Boron fiber is produced by the chemical vapor deposition of boron from boron trichloride on a heated tungsten fiber substrate. Because of the conversion of the tungsten core to a boride during fiber formation a significant residual stress pattern develops in the fiber.[29-31] Tensile stresses are generated in the region of the boride-boron interface which can cause the formation of radial cracks emanating from the interface. These cracks, or just the presence of significant residual fiber stresses, are capable of severely limiting the fiber transverse strength. Both transverse tensile stresses applied during composite mechanical testing and those caused locally during cutting procedures can cause fiber fracture along diametral planes. Larger diameter fibers, having a larger ratio of boron to boride, may be expected to generate smaller tensile residual stresses.[30] Those fibers fabricated by the R. F. technique may also have smaller residual tensile stresses due to the milder thermal gradients at the ends of the reactor hot zone associated with this process. The silicon carbide is expected to have a higher transverse tensile strength due to the fact that the tungsten core is not converted during fiber synthesis.

The transverse tensile strengths of the several different boron and BORSIC fibers discussed above have been measured directly by a diametral compression test technique.[32] The results obtained by this procedure confirm the higher transverse fiber strengths of the larger diameter and R. F. fibers inferred by the composite data presented in Fig. 18.

SUMMARY AND CONCLUSIONS

It has been shown that the transverse elastic modulus of boron aluminum composites is described well by existing formulations based on constituent matrix and fiber moduli. Variations of modulus with test temperature and volume fraction fiber agree with existing predictions.

Composite transverse tensile strength was shown to be related to both the matrix and fiber strengths. This latter quantity varies substantially with fiber type and illustrates the considerable anisotropy of boron fibers. Composite fracture mode, either predominantly matrix failure or fiber splitting, is dependent upon the magnitude of transverse fiber strength relative to matrix strength and controls the functional dependence of composite strength on composite fiber content. Good agreement in strength is obtained with existing analyses when matrix failure predominates.

The sensitivity of composite transverse tensile behavior to fiber edge condition has been demonstrated. Cutting techniques initiate flaws which can propagate and fail the composite specimens during transverse tensile testing. The preexistent splitting tendency of the boron fibers varies with fiber fabrication procedure and determines the susceptibility of the fibers to machining damage.

Significant improvement in composite transverse tensile strength can be achieved by the incorporation of fibers having a high transverse tensile strength. Transverse tensile strengths of up to 45,000 psi can be achieved in this manner. This strength level is approximately a factor of two greater than the strength of boron or BORSIC aluminum composites available at the outset of this research program and has mitigated one of the major impediments to the application of boron-aluminum composites for aerospace applications.

ACKNOWLEDGMENTS

This research was sponsored by Contract F33615-69-C-1539 of the Air Force Materials Laboratory. The help and advice of Capt. D. Rice, program monitor, is greatly appreciated.

The authors would like to thank Mr. L. Dardi for many helpful discussions and technical advice during this research. The help of Messrs. L. Pennington and C. Ramsey is also gratefully acknowledged.

REFERENCES

1. K. Kreider and M. Marciano: *Trans. TMS-AIME*, 1969, vol. 245, p. 1279.
2. J. Mangiapane, *et al.*: Paper No. 68-1037, presented at 5th AIAA Annual Meeting, October 1968.
3. W. Schulz: ASME Paper 71-GT-90, 1971.

4. K. G. Kreider and E. M. Breinan: *Met. Progr.,* 1970, May, p. 104.
5. J. D. Forest and J. L. Christian: *Met. Eng. Quart.,* 1970, vol. 12, p. 1.
6. E. M. Breinan and K. G. Kreider: *Met. Trans.,* 1970, vol. 1, p. 93.
7. E. M. Breinan and K. G. Kreider: *Met. Eng. Quart.,* 1969, vol. 11, p. 5.
8. C. T. Lynch, J. P. Kershaw and B. R. Collins: CRC Critical Reviews in *Solid State Sci.,* November 1970, p. 481.
9. P. E. Chen and J. M. Lin: *Mater. Res. Stand.,* 1969, p. 29.
10. J. M. Lin, *et al.: Polym. Eng. Sci.,* 1971, vol. 11, p. 344.
11. P. W. Jackson, *et al.: J. Mater. Sci.,* 1971, vol. 6, p. 427.
12. M. Basche, *et al.: Fibre Sci. Tech.,* 1968, vol. 1, p. 1.
13. D. Hartog: *Mechanical Vibration,* McGraw Hill, 1956.
14. S. Spinner and R. Valore: *J. Res. Nat. Bur. Stand.,* 1958, vol. 6, p. 459.
15. S. Spinner, *et al.: J. Res. Nat. Bur. Stand.,* 1960, vol. 64A, p. 147.
16. S. Spinner and G. W. Cleek: *J. Appl. Phys.,* 1960, vol. 31, p. 1407.
17. H. J. Stokes: *J. Sci. Inst.,* 1960, vol. 37, p. 117.
18. J. K. Mackenzie: *Proc. Roy. Soc.,* 1950, vol. 63B, p. 2.
19. R. L. Coble and W. D. Kingery: *J. Amer. Cerans. Soc.,* 1956, vol. 39, p. 377.
20. J. G. Kaufman and R. E. Davies: *Mater. Res. Stand.,* 1970, p. 20.
21. D. F. Adams and D. R. Doner: *J. Comp. Mater.,* 1967, vol. 1, p. 152.
22. D. Adams and S. Tsai: *J. Comp. Mater.,* 1969, vol. 3, p. 368.
23. A. Zecca and D. Hay: *J. Comp. Mater.,* 1970, vol. 4, p. 556.
24. J. Ashton, J. Halpin, and P. Petit: *Primer on Composite Materials: Analysis,* Technomic Press, 1969.
25. K. R. Van Horn: *Aluminum,* American Society for Metals, 1967, vol. 2.
26. A. Metcalfe and G. Schmitz: Trans. ASME Paper No. 69-GT-1, 1967.
27. E. Ellison and D. Boon: *J. Less Common Metals,* 1967, vol. 13, p. 103.
28. D. Adams: *J. Comp. Mater.,* 1970, vol. 4, p. 310.
29. F. E. Wawner: *Modern Composite Materials,* Broutman and Crock, eds., Addison-Wesley, 1967.
30. R. Adler, *et al.: Appl. Phys. Lett.,* 1969, vol. 14, p. 354.
31. L. Line and U. Henderson: *Handbook of Fiberglass and Advanced Plastic Composites,* G. Lubin, ed., Van Nostrand, 1969.
32. K. G. Kreider and K. M. Prewo: ASTM Special Technical Publication STP-497, 1972.